



# Cumulative light from the Epoch of Reionization - the Near Infrared Background and the 21cm line

Elizabeth R. Fernandez<sup>1</sup>, Saleem Zaroubi<sup>1</sup>, and Ilian T. Iliev<sup>2</sup>

<sup>1</sup> Kapteyn Astronomical Institute, The University of Groningen, Landleven 12, 9747 AD Groningen, The Netherlands, e-mail: E.Fernandez@astro.rug.nl

<sup>2</sup> Astronomy Centre, Department of Physics & Astronomy, Pevensey II Building, University of Sussex, Falmer, Brighton BN1 9QH, United Kingdom

**Abstract.** Observations of the Epoch of Reionization are now becoming a distinct possibility. High-redshift galaxy surveys are discovering galaxies well into the Epoch of Reionization. However, these observations present a small portion of the total picture, providing information on only the brightest objects within the survey. I will discuss two other observations that can reveal information on reionization history. Cumulative light from all galaxies, including those numerous galaxies below the detection limit of high redshift galaxy surveys, would be present in the Near Infrared Background. Emission from the 21cm line would originate from neutral areas in the IGM, and would be reveal information about the early stages of reionization. I will present theoretical modeling of both the 21cm line and the Near Infrared Background, and show how these two observations are correlated. This can help reveal information about the buildup of galaxies, their stellar populations, and reionization history.

**Key words.** cosmology: early Universe, observations, theory – infrared:galaxies – galaxies:high redshift

## 1. Introduction

The first generations of stars could have been very different than those we observe today. Because metals are generated by stellar processes, these stars would have been metal free, and possibly be on the order of hundreds of solar masses. As these stars died, the Intergalactic Medium (IGM) became enriched with metals. At some point, a critical metallicity was reached, and metal-poor Population II stars began to form. These Population II stars could have been smaller than their Population III pro-

genitors, since the presence of metals in the IGM would have allowed the gas cloud to fragment into smaller massed stars. Currently, it is unknown when this critical metallicity was reached, or how long this transition took.

As star formation continued throughout this universe, the entirety of neutral hydrogen was ionized, in a process called reionization. Since stars would have created an abundant source of ionizing photons, if we can interpret the process of reionization, we can also come to an understanding of the stars doing the ionizing.

Today, observations of the Epoch of Reionization are becoming more and more common, and there is great promise to extract information from these observations. Here, we discuss two of these observables. The cumulative light of ultraviolet photons at  $z \sim 10$ , those which are responsible for reionization, will be redshifted, and therefore they must make up at least some portion of the background in the infrared. In addition, the hydrogen in areas that have not yet been affected by star formation will still be neutral and will emit 21cm emission. This emission will be concentrated at high redshifts, and areas where star formation has not yet ionized the regions around it. We discuss these two observables, and how we can use them to extract more information on the first stars and reionization history.

## 2. The Population III to Population II transition and the NIRB

Ionizing photons from the Epoch of Reionization will be redshifted, and therefore, should make up at least some portion of the Near Infrared Background (NIRB). The intensity of these high redshift stars is given as:

$$I_\nu = \frac{c}{4\pi} \int \frac{dz p([1+z]\nu, z)}{H(z)(1+z)} \quad (1)$$

(Peacock 1999). Therefore, the intensity depends on the emissivity  $p([1+z]\nu, z)$  of high redshift stars, which is sensitive to the properties of the stars themselves, such as their luminosity, lifetime, mass, and star formation rate. For more information on the computation of the intensity, please refer to Fernandez & Zaroubi (2013) and Fernandez & Komatsu (2006). Then, in order to model the star formation rate  $\dot{\rho}_*(z)$ , we approximate a fit as:

$$\dot{\rho}_*(z) = 10^{y_0 + y_1 z + y_2 z^2}, \quad (2)$$

where  $y_1 = -0.03$ , and  $y_2 = -0.004$ . The value of  $y_0$  is then set so that the star formation rate at  $z = 6$  is  $0.02 \text{ M}_\odot \text{ yr}^{-1} \text{ Mpc}^{-3}$ , from theoretical approximations (Alvarez et al. 2012; Johnson et al. 2013), and slightly higher than current observational constraints from gamma-ray bursts (e.g. Kistler et al. 2009; Robertson

& Ellis 2012). This model is not meant to be physical, but instead it approximates the star formation rate to be consistent with results from Trenti & Stiavelli (2009), Alvarez et al. (2012), and Johnson et al. (2013).

In order to describe the gradual transition from Population III to Population II stars, we describe the fraction of stars that are Population III stars ( $f_p$ ) by:

$$f_p = \frac{1}{2} [1 + \text{erf}(\frac{z - z_t}{\sigma_t})] \quad (3)$$

(Cooray et al. 2012), where the redshift where the transition from Population III stars to Population II stars is half complete is  $z_t$  and the length of this transition is parameterized by  $\sigma_t$ . Changing these parameters can model various enrichment histories. The escape fraction is then set to be consistent with photon starved reionization. We allow star formation to begin with only Population III stars with a heavy Larson mass spectrum. Star formation then transitions to Population II stars with a Salpeter mass spectrum. Currently, we do not know when this transition occurred. In Figure 1, we allow this redshift of transition ( $z_t$ ) to be either 8, 10, 12, or 15. Massive Population III stars will have very strong nebular features, such as the Lyman- $\alpha$  line. These nebular features could have a higher intensity than less massive Population II stars at lower redshift. Therefore, a presence of a 'bump' in the cumulative spectra of the NIRB could be indicative of the strong Lyman- $\alpha$  line resulting from Population III stars that could have existed to lower redshift.

To model the possibility that Population III stars might not be as massive, we computed the spectrum of the NIRB when Population III stars are a variety of masses, shown in Figure 2. When Population III stars are more massive, their associated Lyman- $\alpha$  line is stronger, and the associated bump from the Population III epoch is stronger. This bump is reduced if Population III stars are less massive, and vanishes if Population III stars are no more massive than Population II stars. Therefore the presence of a Lyman- $\alpha$  bump would be the hallmark of a massive Population III era that persisted to late times.

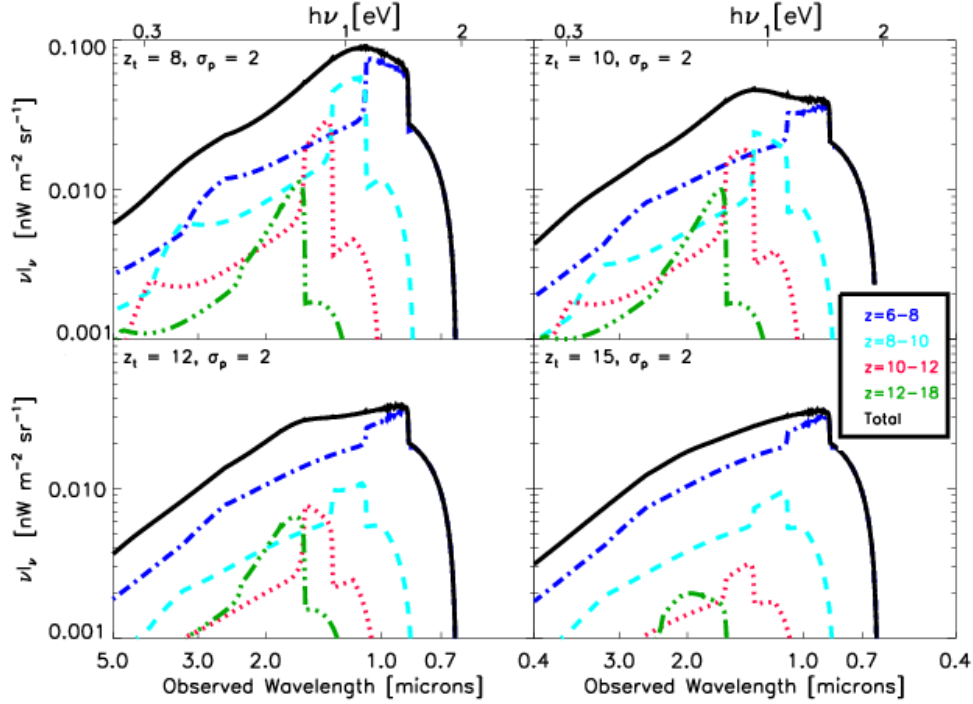


**Fig. 1.** The spectra of the NIRB from stars above a redshift of 6. In each panel, we show a different redshift of transition  $z_t$ , which quantifies when the majority of star formation transitioned from Population III to Population II. If Population III stars persist to lower redshifts ( $z_t$  is relatively low) a 'bump' in the spectra is seen from the end of the Population III epoch, a product of the strong Population III Lyman- $\alpha$  line. The solid lines are the total contribution from  $z = 6 - 30$ , dot-dashed are  $z = 6 - 8$ , dashed are  $z = 8 - 10$ , dotted are  $z = 10 - 12$ , and dashed-triple dot are  $z = 12 - 18$ .

### 3. Cross-Correlations of the Near Infrared Background and the 21cm Emission

More information about high redshift stars can be found by combining observations - namely, observations of both the Near Infrared Background and observations of 21cm emission. Since emission in the NIRB results from areas of star formation, it should originate from different regions than 21cm emission, which results from areas of neutral hydrogen which have not been ionized by star formation. Therefore, these observations should be anti-correlated.

We create simulated sky maps that can mimic observations in the infrared and observations of the 21cm line, predicted to be observed by LOFAR. We begin with N-body simulations with radiative transfer (Iliev et al. 2013). The star formation in small halos ( $10^9 M_\odot$  to  $10^8 M_\odot$ ) is suppressed when it occurs close to larger halos. These simulations, paired with analytical formalisms, can predict the emission of both the emitting halos and the neutral regions that have yet to be ionized by star formation. For our model, we assume that stars are Population II stars with ( $Z = 1/50 Z_\odot$ ), and a Salpeter mass function.

To calculate the 21cm brightness temperature, the density and ionization fraction of the

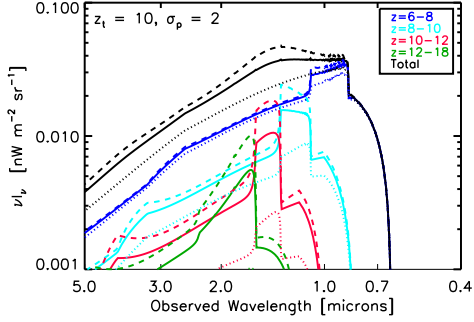


**Fig. 2.** The spectrum of the NIRB when Population III stars have various masses. In each case, the Population II stars have a Salpeter mass spectra. These are combined with Population III stars with a very heavy Larson mass spectrum (on the order of  $250M_{\odot}$  - dashed lines), Population III stars with a light Larson mass spectrum (on the order of  $10M_{\odot}$  - solid lines), and Population III stars with a Salpeter mass spectrum (dotted lines).

IGM are used from the simulation. The brightness temperature is then:

$$\delta T_B \sim 28.5 \left[ \frac{1+z}{10} \right]^{1/2} (1+\delta) \times \left( \frac{\Omega_B}{0.042} \frac{h}{0.73} \right) \left( \frac{0.24}{\Omega_m} \right)^{1/2} \text{ mK}, \quad (4)$$

(Field 1959) where the value of  $\delta T_b$  depends on the overdensity of neutral hydrogen,  $1 + \delta$ .

By combining the simulations and the analytical formulas, we construct line of sight maps, simulating observational fields for both the NIRB and the 21cm emission. The cross-correlation is then calculated using the Pearson correlation coefficient:

$$\rho_{21cm, NIRB} = \frac{\text{cov}(\delta T_b, I_{NIRB})}{\sigma_{\delta T_b} \sigma_{I_{NIRB}}}. \quad (5)$$

The cross-correlation for the entire NIRB and LOFAR map is shown in Figure 3. The two populations are very strongly anti-correlated, as expected. The error bars are determined from cross-correlating the 21cm map with 1000 realistic realizations of a randomized map of the NIRB.

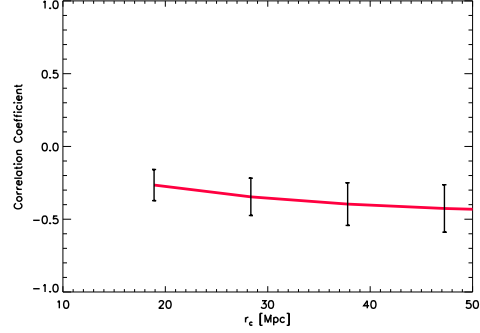


**Fig. 3.** The cross correlation of the entire NIRB map against redshift slices of the 21cm background maps.

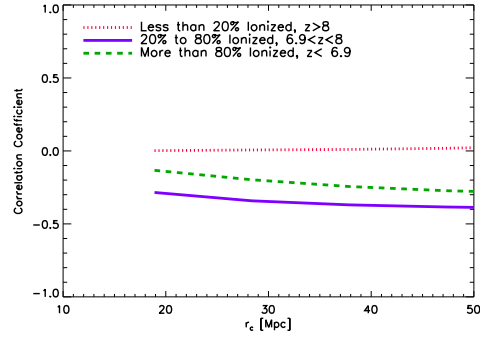


**Fig. 4.** The correlation coefficient of the entire NIRB against three slices of the 21cm emission - when the universe is less than 20% ionized (early times,  $z > 8$ ), when the universe is more than 80% ionized (late times,  $z < 6.8$ ), and mid-reionization. The strongest anti-correlation results when the universe is partially ionized.

Since the 21cm emission is line emission, the entire NIRB map can also be cross-correlated with only certain slices of the 21cm LOFAR map. The results are shown in Figure 4. Here, we can see that the cross-correlation is the strongest when the ionization fraction is about 50% (Fernandez et al. 2014).

## 4. Conclusions

Backgrounds could prove to be a very useful way to constrain the Epoch of Reionization. These backgrounds can provide information on

the stars themselves and the reionization history of the Universe. The Near Infrared Background from high redshift stars is the cumulative redshifted light from reionization. The spectra of the Near Infrared Background can show evidence of a massive Population III era that persisted to late times if this spectra contains a bump from the strong Lyman- $\alpha$  emission from massive Population III stars (Fernandez & Zaroubi 2013). The NIRB can also be cross-correlated with the 21cm background emission, emission resulting from neutral hydrogen in areas where star formation is not occurring. This emission is anti-correlated with the NIRB, since these emissions result from different areas. This anti-correlation is strongest when the ionized fraction is about 50% (Fernandez et al. 2014).

## References

- Abel, T., Bryan, G. L., & Norman, M. L. 2002, *Science*, 295, 93
- Alvarez, M. A., Finlator, K., & Trenti, M. 2012, *ApJ*, 759, L38
- Cooray, A., et al. 2012, *ApJ*, 756, 92
- Fernandez, E. R., & Komatsu, E. 2006, *ApJ*, 646, 703
- Fernandez, E. R., Zaroubi, S., Iliev, I. T., Mellema, G., & Jelić, V. 2014, *MNRAS*, 440, 298
- Fernandez, E. R., & Zaroubi, S. 2013, *MNRAS*, 433, 2047
- Field, G. B. 1959, *ApJ*, 129, 536
- Iliev, I. T., et al. 2013, *ArXiv e-prints*:1310.7463
- Johnson, J. L., Dalla, V. C., & Khochfar, S. 2013, *MNRAS*, 428, 1857
- Kistler, M. D., et al. 2009, *ApJ*, 705, L104
- Peacock, J. A. 1999, *Cosmological Physics*, (Cambridge Univ. Press, Cambridge)
- Robertson, B. E., & Ellis, R. S. 2012, *ApJ*, 744, 95
- Trenti, M., & Stiavelli, M. 2009, *ApJ*, 694, 879